1

Metallic Nanoparticles Coupled with Photosynthetic Complexes

Sebastian Mackowski
Optics of Hybrid Nanostructures Group
Institute of Physics, Nicolaus Copernicus University, Torun
Poland

1. Introduction

Plasmon excitations in metallic nanoparticles provide an efficient way to manipulate electromagnetic fields at the nanoscale (Maier, 2004). While the interactions between plasmons and simple nanostructures such as organic dyes or semiconductor nanocrystals is relatively well described and understood, application of metallic nanoparticles to multi-pigment structures has started just recently (Carmeli, 2010; Govorov, 2008; Kim, 2011; Mackowski, 2008; Nieder, 2010). Light-harvesting complexes, or more generally, photosynthetic complexes, are quite appealing in this regard as they not only provide an interesting biomolecular system for studying plasmon effect on both the optical properties of pigments and the energy transfer between them, but also they could offer attractive potential application route in photovoltaics (Atwater & Polman, 2010; Mackowski, 2010).

Extending concepts and methods that have been developed for describing the coupling of single organic chromophores with plasmon excitations in metallic nanoparticles (Anger, 2006; Chettiar, 2010; Govorov, 2006) to multi-chromophoric biological systems has not been completely straightforward from both theoretical and experimental points of view. On the one hand, organic molecules or semiconductor quantum dots are much more robust nanostructures than pigment-protein complexes, therefore, the sample preparation in the latter case should be more gentle, so that the protein itself maintains its structure. Preserving protein structure implies that the function of the complex as a whole also remains intact. This assures conservation of the energy transfer pathways between various chromophores comprising the complex as well as identical optical properties, including absorption and fluorescence, to that of the isolated (decoupled from a metallic nanoparticle) biomolecule. On the other hand, from the theory standpoint, biomolecules, and in particular light-harvesting complexes, render themselves a real challenging system to model due to multitude of interactions between chromophores such as chlorophylls and carotenoids (Blankenship 2002), which results in many energy transfer pathways and formation of strongly coupled excitonic systems, as well as conformational changes of the protein itself. Nevertheless, driven by the continuous development of optical spectroscopy and microscopy techniques (Polivka & Sundstom 2004) as well as more efficient modeling tools, significant progress has been achieved in understanding interactions and functions of light-harvesting complexes. It has also been helped by high-resolution crystal structures of the

complexes (Hofmann 1996; McDermott, 1995), enabling thus direct association of the pigments as well as their interactions both with themselves and the protein with the actual structure and spatial arrangement of the pigments in these systems.

The purpose of this chapter is to review recent research carried out on hybrid nanostructures composed of metallic nanostructures and light-harvesting complexes. In general, the research is focused on improving the light absorption of the light-harvesting complexes through properly designed plasmonic nanostructures. However, before we start discussing particular hybrid nanostructures fabricated in the context of plasmonically enhanced absorption of light-harvesting complexes, we describe two basic concepts of metal-enhanced fluorescence: distance dependence of the fluorescence intensity and the influence of spectral properties of metallic nanoparticles and placed nearby molecules (Anger, 2006). This brief introductory discussion is essential for understanding the rationale behind designing hybrid nanostructures that involve biological fluorescing complexes.

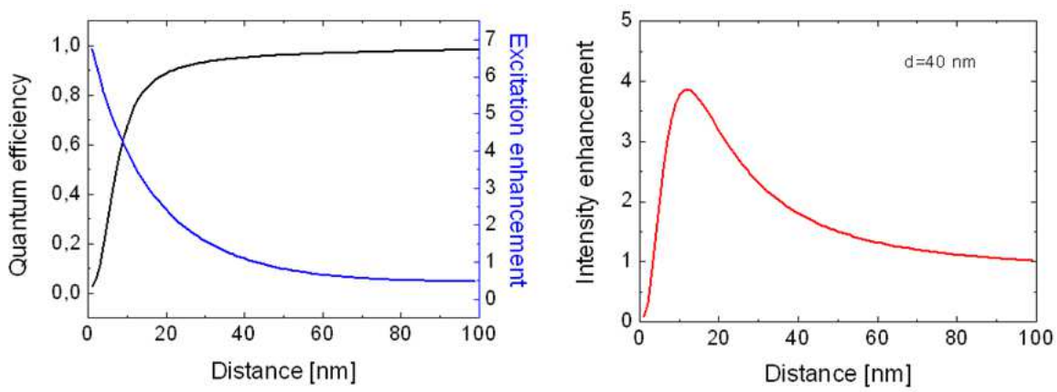

Fig. 1. Dependence of the quantum yield and non-radiative fluorescence quenching upon the distance. Fluorescence intensity of a chromophore displayed as a function of the distance between the chromophore and spherical metallic nanoparticle with 40 nm diameter.

The optical properties of a fluorophore placed in the vicinity of a metallic nanoparticle are strongly affected by plasmon excitations induced in the latter by a laser light. Without a metallic nanoparticle, a fluorophore is characterized with three rates: absorption rate, radiative rate, and non-radiative rate. Since the oscillation of electrons in the metallic nanoparticle results in creation of local electromagnetic field, in principle all three rates can be changed (Lakowicz, 2006). In addition, another process related to non-radiative energy transfer from the fluorophore to the metallic nanoparticle could also take place in such a hybrid nanostructure. The influence of plasmon excitations upon the quantum yield of a fluorophore and non-radiative energy transfer between the fluorophore and metallic nanoparticle has been recently studied theoretically. In particular, the dependence on the separation distance between the two nanostructures has been analyzed in detail. It turns out that the distance between the fluorophore and metallic nanoparticle is of critical importance in regard to the process that plays dominant role in such a system. In Fig. 1 we show the dependence of the excitation rate and quantum efficiency of a fluorophore upon the distance to the metallic nanoparticle. In this example we consider a metallic nanoparticle with diameter of 40 nm**.** The excitation efficiency increases exponentially with reducing the distance, which is a clear manifestation of stronger electromagnetic field felt by the

fluorophore due to plasmon excitation in the metallic nanoparticle. On the other hand, the quantum efficiency, when approaching the range of distances shorter than 20 nm, starts to drop significantly, due to the non-radiative energy transfer from the fluorophore to the nanoparticle. The net result of these two processes in displayed in Fig. 1, where a clear non-monotonic dependence of the intensity of fluorescence emitted by the fluorophore upon the distance to the metallic nanoparticle can be seen. Importantly, the strongest plasmon induced enhancement of the fluorescence occurs for distances between 10 and 30 nm; for smaller distances non-radiative fluorescence quenching dominates, while for longer distances the fluorophore barely feels the presence of the metallic nanoparticle.

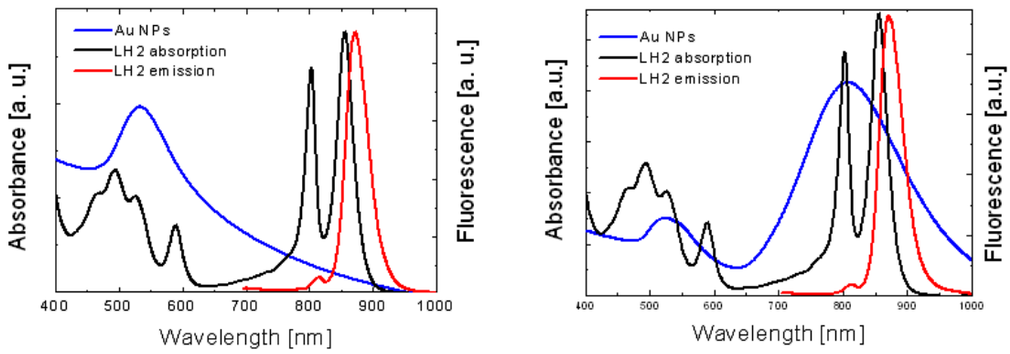

Fig. 2. Comparison between absorption spectra of spherical end elongated gold nanoparticles with the fluorescence and absorption of the LH2 complex. In the first case plasmon excitations should influence mainly the absorption in the visible range, in the second case the effect should be visible for absorption and emission in the infrared.

Another critical parameter that influences the interaction between metallic nanoparticle and fluorophore is the relation of their spectral properties. This is shown schematically in Fig. 2. In the first case scenario the absorption of metallic nanoparticles overlaps significantly with absorption of a biomolecule (in this case this is the LH2 complex from purple bacteria) in the spectral range of about 530-550 nm, while featuring virtually no overlap with the fluorescence. One may expect that for such a combination the major influence of metallic nanoparticles is due to absorption enhancement. In contrast, for a hybrid nanostructures built of components characterized with spectral properties as those displayed in Fig. 2b, there should be absorption enhancement both around 560 nm as well as in the infrared spectral region, around 800 nm. In addition, since there is a spectral overlap between plasmon band and fluorescence emission, the radiative rate should also increase as a result of plasmon excitation.

Optical spectroscopy provides variety of techniques that allows for distinguishing between various processes that determine the net effect of plasmonic excitations in metallic nanoparticles on a fluorophore. Indeed, in an ideal situation, where only absorption rate is affected by the plasmon excitation, there should be no change in the fluorescence decay time, while an additional band should appear in the fluorescence excitation spectrum. In contrast, when only radiative rate increases as a result of plasmon coupling, the fluorescence excitation spectrum for a hybrid nanostructure should be identical to the reference structure, with much shorter fluorescence decay time. Several experimental configurations exhibiting these various aspects of plasmon coupling with pigment – protein complexes are discussed in this contribution.

2. Materials and methods

In this section we introduce the structure and the optical properties of light-harvesting complexes used in our studies as well as present basic characteristics of metallic nanostructures, including their morphology and plasmon characteristics. Next we present experimental techniques employed for investigating the interactions between plasmon excitations and chromophores embedded in the proteins. These include standard absorption and fluorescence/fluorescence excitation spectroscopy, both in solution and in a layered geometry, as well as confocal fluorescence microscopy coupled with time-resolved capability and spectrally-resolved detection. Combination of all these experimental techniques allows for comprehensive description of plasmon-induced effects on the complex biomolecular systems.

2.1 Light-harvesting complexes

Pigment-protein complexes that take part in photosynthesis can be generally divided into two groups: complexes containing reaction centers, which carry out charge separation, and complexes responsible solely for harvesting the sunlight and transferring it to the reaction centers. Large proteins of Photosystem I and Photosystem II fall into the first category, while light harvesting complex 2 (LH2) from purple bacteria and peridinin – chlorophyll – protein (PCP) complex from algae belong to the second group. As the structure and function of all these biomolecules has been described in detail previously, we focus here only on the aspects that are relevant for understanding the influence of plasmon excitations on the optical properties of light-harvesting systems, PCP and LH2.

2.1.1 Peridinin-chlorophyll-protein

Light-harvesting complexes were developed in the course of evolution in order to enhance and broaden the absorption of photosystems for the efficient use of sunlight in photosynthesis. Their major function of these pigment-protein complexes is to harvest the sunlight and transfer the energy to the Photosystems. Peridinin-chlorophyll-protein (PCP) found in Dinoflagellates *Amphidinium carterae* is one of many such complexes. It is a water-soluble protein employed as an antenna external to the membrane. The structure of the PCP complex, shown in Fig. 3, has been determined with 1.3 Å resolution using X-ray crystallography (Hofmann, 1996). The native form of PCP consists of two chlorophyll a (Chl) and eight peridinin (Per) molecules embedded in a protein matrix. All the pigments are arranged in two almost similar clusters and embedded in the hydrophilic protein capsule. The conjugated portion of each Per is close to the chlorophyll tetrapyrrole ring at a van der Waals distance (3.3 to 3.8 Å), the distance between Mg atoms of the two Chl a in one monomer is 17.4 Å and intercluster edge-to-edge distances between Per are in the range of 4-11 Å. The ratio of Per to Chl a of 4:1 indicates that PCP utilizes the carotenoids as its main light-harvesting pigments. It has been shown that the PCP complex can be reconstituted with other Chl derivatives which exhibit different optical properties (Brotosudarmo, 2006). Importantly, the folding of the protein used in the reconstitution procedure takes place over almost identical pathway as in the native system, which results in very similar structures of the reconstituted systems. Since each of these chlorophyll molecules features specific absorption and emission characteristics, it became possible to construct and study the

energy transfer dynamics as well as inter-pigment interactions in a well-defined geometry given by the protein (Mackowski, 2007, Polivka, 2005).

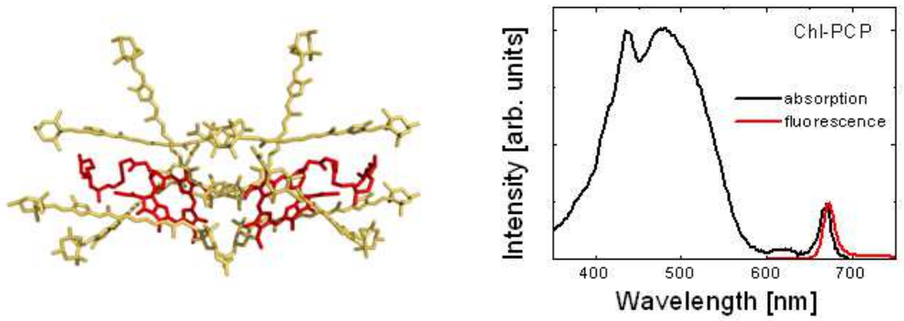

Fig. 3. Pigment structure of the PCP complex reconstituted with Chl *a* together with absorption (black line) and fluorescence (red line) measured in water solution at room temperature.

The absorption spectrum of the Chl-PCP displayed in Fig. 3 has an intense, broad band between 400 to 550 nm that is mainly due to Per absorption, and two Chl – related bands at 440 nm (Soret) and 660 nm (Q_Y). One example of chlorophylls used for reconstituting PCP complexes is [3-acetyl]-chlorophyll a (acChl). Chemically, it differs from Chl only by the C-3 substituent, but the absorption and fluorescence spectra of acChl-PCP, the PCP complex reconstituted with acChl, are red shifted as compared to the PCP complex containing Chl. At the same time the Per absorption in the blue-green spectral range is affected very slightly. For the PCP complexes reconstituted with acChla the absorption of the Qy band of the chlorophyll molecules is shifted by approximately 20 nm to the red. The fluorescence emission of the PCP complex originates from weakly coupled Chl molecules and it appears at 670 nm for Chl-PCP and 690 nm for acChl-PCP. Upon absorption of light, peridinins in PCP transfer their electronic excitation to Chl a. The efficiency of this excitation energy transfer is higher than 90% [20]. Subsequently, Chl a passes the energy on to membrane-bound light-harvesting complexes and the Photosystem II. Clearly, the absorption spectrum of PCP enables the photosynthetic apparatus to harness the sunlight not only in the red spectral range, but it extends it into the blue-green spectral region.

Optical spectroscopy studies of both native and reconstituted PCP complexes have been carried out on the ensemble (Akimoto, 1996; Kleima, 2000; Krueger, 2001) and single-molecule levels (Mackowski, 2007; Wormke, 2007a; Wormke, 2008). Using transient absorption in femtosecond timescale main energy transfer pathways have been described, it has also been demonstrated that the two Chl a molecules interact relatively weakly with characteristic transfer time between them to be of the order to 12 ps (Kleima, 2000). These observations were also corroborated with fluorescence studies of individual PCP complexes: it has been shown that it is possible to distinguish emission originating from each of the two Chl a molecules and using the property of sequential photobleaching of the Chl the energy splitting between the two molecules in the monomer were determined (Wormke, 2007a). Recent work on PCP complexes reconstituted with both Chl a and Chl b provided coherent description of the energy transfer pathways and dynamics in this unique antenna (Mackowski, 2007).

2.1.2 Light-harvesting complex 2

Another example of a pigment-protein complex employed to harness sunlight energy and transfer it efficiently to reaction centers is a light-harvesting complex 2 (LH2) from purple bacteria Rhodopseudomonas palustris. This protein is placed in the thylakoid membrane, where many of LH2 complexes surround relatively widely spaced LH1 complexes, to which they transfer excitation energy. The BChl a molecules in LH1 have a single strong near-infrared absorption band of 875 nm, while LH2 has two strong BChl a absorption bands at 800 nm and 850 nm (Fig. 2). In this way the energy gradient is formed, which facilitates efficient energy transfer from LH2 to LH1 complex, and then further to the reaction center. Both the structure and the optical properties of the LH2 have been a subject of intense studies in recent years (van Oijen, 1999; Hofmann, 2003; Bopp, 1997). It has been shown using atomic force microscopy technique, that LH2 complexes arrange around a LH1 light-harvesting complex, in the middle of which is a reaction center (Scheuring, 2004). The spatial arrangement of Bacteriochlorophylls (BChls) and carotenoids in this complex is displayed in Fig. 4. The X-ray crystallography studies of the LH2 complex have shown that out of the 27 BChl molecules 18 form a strongly coupled ring with average distances between the molecules less than 1 nm (McDermott, 1995). This excitonically coupled ring is responsible for the absorption band at 850 nm. The remaining 9 molecules form a ring of weakly coupled BChls as they are spaced by more than 2 nm. All pigments, BChls and carotenoids, are embedded in a hydrophobic protein (not shown). Single molecule investigations (van Oijen, 1999) proved that the B 850 ring are in fact not fully symmetric, and the exciton levels feature significant splitting.

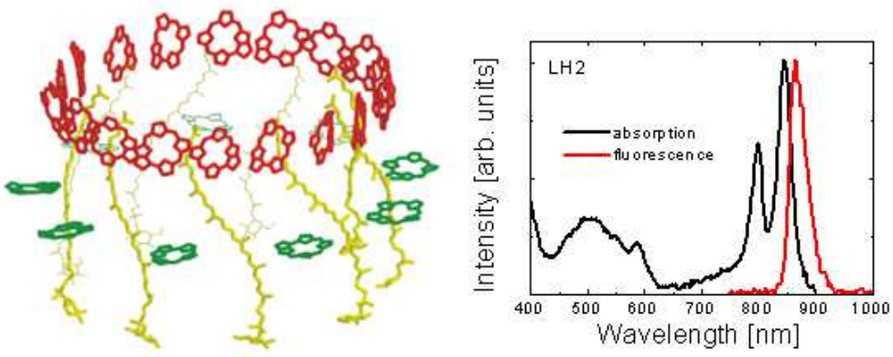

Fig. 4. Pigment structure of the LH2 complex together with absorption (black line) and fluorescence (red line) measured in buffer solution at room temperature.

The absorption spectrum of the LH2 complex is shown in Fig. 4. It consists of two prominent bands at 800 nm and 850 nm which correspond to absorption of the two rings of BChl molecules. The carotenoids are in close contact with both BChl rings, and are mainly responsible for a broad absorption between 390 nm and 550 nm. Importantly, the fluorescence of LH2, which originates exclusively from the strongly coupled ring (named B850) has therefore an excitonic character. The presence of strong absorption bands and fluorescence emission in the infrared spectral range requires – in order to influence the optical properties of the LH2 complex - application of metallic nanoparticles that feature plasmon resonances in the near infrared.

2.2 Metallic nanostructures

Metallic structures with nanometric sizes have been the subject of intense research in recent years due to mainly unique optical properties of these systems that can be used for manipulating light at the nanoscale, designing biosensors and artificial chiral nanostructures, enhancing the optical properties of semiconductor nanocrystals and organic fluorescent dyes, enabling detection of emitters characterized with low fluorescence quantum yields, such as carbon nanotubes or DNA. In addition to efforts aimed at exploiting plasmon effect in metallic nanoparticles, significant research have been carried out to achieve almost perfect control of the morphology of metallic nanoparticles, and thus the plasmon properties thereof. Among many techniques of fabrication of metallic nanostructures are evaporation of metallic film on a corrugated substrate (Chettiar, 2010; Mackowski 2008), nanosphere lithography (Hulteen, 1995), electron beam lithography, electrochemical deposition, direct formation of silver island film (Ray, 2006), and chemical synthesis (Link, 1999). Each of these methods requires particular technical capabilities, frequently the experimental setups for nanostructure fabrication is expensive making them hardly accessible. Chemical synthesis of nanoparticles however, is quite simple, at least on the basic level, and, when mastered, provides a way to obtain highly monodisperse nanoparticles with tailored morphology and surface functionalization. This results in well-defined optical properties such as energies of plasmon resonances, and conjugation capabilities to other nanostructures or surfaces. In this contribution we describe the interactions present in hybrid nanostructures composed of light-harvesting complexes PCP and LH2 and metallic nanostructures fabricated using chemical deposition of silver island film on a glass substrate, electron beam assisted deposition of silver island film on a glass substrate, as well as chemically synthesized gold spherical nanoparticles and nanorods. We show that by careful design of a hybrid nanostructure we can control the impact of plasmon excitations in metallic nanoparticles upon the absorption and emission of the chlorophyll-containing light-harvesting complexes.

2.2.1 Silver island film

One of the simplest to fabricate metallic nanostructures is a corrugated metallic film. The method to obtain such a film with islands characterized with sizes of tens of nanometers has been previously applied to study the impact of plasmon interactions upon the fluorescence of various organic dyes, semiconductor quantum dots, and a few proteins, including the green fluorescent protein (Lakowicz, 2006; Ray, 2006). Silver island films used in our experiment were prepared by reducing an aqueous silver nitrate solution. All chemicals were purchased from Sigma-Aldrich and used as received. First, freshly prepared aqueous NaOH (1.25 M) was added to a silver nitrate solution. The precipitate was re-dissolved by adding NH_4OH, and the solution was cooled to ~5°C under stirring. After adding D-glucose, clean microscope cover slips were dipped in the solution, which was then heated up to 30°C. The resulting Ag-covered glass coverslips were examined using absorption spectroscopy and atomic force microscopy (AFM). In order to change the morphology and thus the properties of the silver island film, we fabricated several samples with varied dipping time in the reaction solution: the coverslips were kept in solution for 1 and 3 minutes. In Fig. 5 we show AFM image of the SIF obtained by dipping the coverslip for 1 minute in the reaction solution. The islands are characterized with average sizes of about 40-

50 nm laterally and the surface density is very high. In addition we also include in Fig. 5 the absorption spectrum measured for the SIF structure which features plasmon resonance with a maximum at 450 nm and the linewidth of about 150 nm, and thus matches the absorption of Per in the PCP complexes.

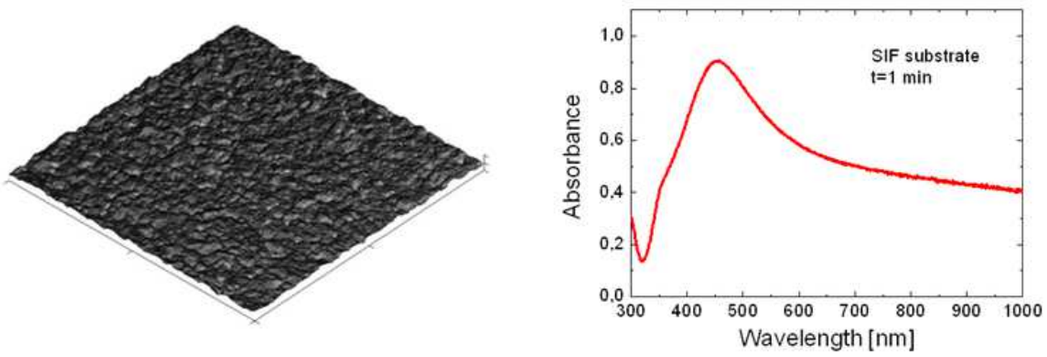

Fig. 5. Atomic force microscopy image of a silver island film fabricated by chemical synthesis together with absorption spectrum of the sample obtained for 1 minute-long dipping time of the glass substrate in the reaction solution. The lateral size of the AFM image is 5 microns.

2.2.2 Semicontinuous metallic layer

The semicontinuous silver film has been fabricated using electron beam-assisted evaporation of silver on glass substrate (Chettiar, 2010). While this nanostructure may look similar to the SIF discussed above, the substrates obtained with the e-bam technique are typically more homogeneous, the sizes and shapes of the silver islands is controlled to higher degree. Proper adjustment of the parameters during the evaporation process leads to corrugated metallic films with designed optical properties. For instance, it has been shown that by changing evaporation time it is possible to obtain morphologies ranging from roughly isolated islands to the strongly coalescing ones. Such differences in morphology resulted in strong shift of plasmon energies towards the red and near infrared spectral ranges, opening thus completely new possibilities for applying these structures for controlling the optical properties of infrared – emitting systems. Yet another important advantage of semicontinuous metallic films fabricated using e-beam assisted evaporation is the capability of uniform coating of such films with dielectric layers with thicknesses ranging from a few nanometers up to tens of nanometers. As plasmon induced effects depend crucially upon the separation between metallic nanoparticles and optically active molecules, such structures render themselves a highly suitable system for investigating processes that occur in plasmonic hybrid nanostructures. In particular, the results included in this contribution have been obtained for a semicontinuous silver film covered with a 25-nm-thick SiO_2 layer evaporated in the same process without exposing the structure to ambient conditions.

2.2.3 Colloidal metallic nanoparticles

Among metallic nanostructures, ones of the most studied are colloidal metallic nanoparticles. It is triggered mainly by enormous variety of metallic nanoparticles that can

be synthesized, even with little resources: sizes of the nanoparticles range from a few to a few hundreds of nanometers. They can also be of essentially any shape: spherical, elongated, triangular, cube or star-like. Furthermore, since the nanoparticles are synthesized in the colloidal form, it is possible to functionalize their surface with functional group suitable for specific attachment to surfaces or conjugation with other nanostructures. Lastly, there have been many examples for self assembly of metallic nanoparticles in complex structures with new properties and functions (Link, 1995).

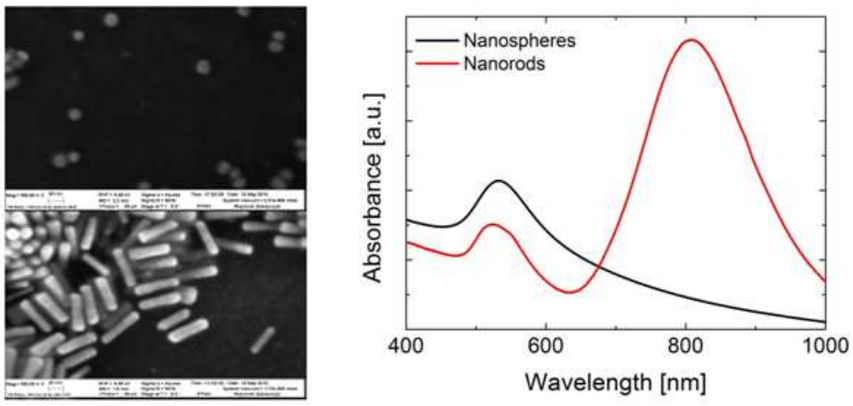

Fig. 6. Scanning electron microscopy images of gold spheres and nanorods. The structural data is accompanied with absorption spectra measured for these two samples at room temperature.

In this contribution we report on synthesis of spherical gold nanoparticles and gold nanorods with the purpose to match absorption bands of light-harvesting complexes. While spherical gold nanoparticles, which feature plasmon resonances around 500-500 nm correspond to carotenoid absorption both in the PCP and LH2 complexes, the nanorods have their resonance also in the infrared, as shown in Fig. 6. By controlling the reaction we tune the energy of the plasmon resonance exactly to 800 nm, thus matching perfectly the B800 absorption of the LH2 complex.

Gold nanoparticles were synthesized using a reduction reaction and dispersed in toluene. The average diameter of the nanocrystals was 5 nm, which results in a plasmon resonance maximum at 530 nm. The synthesis of Au nanorods was based on seed-mediated growth in water solution. All chemicals ($HAuCl_4 \times 3H_2O$ (99.9%), $NaBH_4$ (99%), L-Ascorbic Acid (99+%), hexadecyltrimethylammoniumbromide (CTAB) (99%), and $AgNO_3$ (99+ %)) were purchased from Aldrich and used without further purification. Deionized water (Fluka) was used in all experiments. In order to prepare Au seeds CTAB solution (4.7 ml, 0.1M) was mixed with 25 µl of 0.05 M $HAuCl_4$. To the stirred solution, 0.3 ml of 0.01 M $NaBH_4$ was added, which resulted in the formation of brownish yellow solution. Seeds solution was kept at room temperature until further used. For the synthesis we use Au seeds prepared beforehand. The "seed-mediated" method was developed previously; it is carried out in aqueous solution at atmospheric pressure and near room temperature. Appropriate quantities and molarities of CTAB (150 ml, 0.1 M), $HAuCl_4$ (1.5 ml, 0.05 M), L-Ascorbic acid (1.2 ml, 0.1 M), 0.01 M $AgNO_3$ (1.6 ml, 1.8 ml, 2 ml) and seed (360 µl) water solutions were added one by one in a flask, followed by a gentle mixing. Addition

of ascorbic acid, as a mild reduction agent, triggered a mixture color change from dark yellow to colorless. After addition of the seed solution, the mixtures was put into water bath and kept at constant temperature of 28 ^{o}C for 2 hours. Obtained products were separated from unreacted substrate and spherical particles by centrifugation at 9.000 rpm for 60 minutes. The supernatant was removed using a pipette and the precipitate was redissolved in pure water.

2.3 Sample preparation

In the research described in this work, we have used several sample architectures, from a very simple ones, where light-harvesting complexes were deposited directly on the surface of the metallic layer being either in the form of silver island film or colloidal gold nanoparticles spin-coated on a glass coverslide, to more advanced, where metallic nanoparticles were separated from the light-harvesting complexes by a thin dielectric layer. For that purpose we used SiO2 deposited using e-beam assisted evaporation, the thickness of the SiO2 layer was changed from 5 nm to 40 nm. The light-harvesting complexes were dispersed in a PVA and then spin-coated on the substrate.

2.4 Experimental techniques

The optical properties of hybrid nanostructures comprising light-harvesting complexes and metallic nanostructures have been studied using absorption and fluorescence spectroscopy in the visible and infrared regions. spectral region. Absorption spectra were obtained using a Cary 50 spectrophotometer. Fluorescence and fluorescence excitation spectra of both structures were measured using the FluoroLog 3 spectrofluorimeter equipped with specially designed mount suitable for holding planar samples. A Xenon lamp source with a double grating monochromator was used for excitation and the signal was detected with a thermoelectrically cooled photomultiplier tube characterized by a dark current of less than 100 cps.

Fluorescence spectra of samples comprising light-harvesting complexes and Au nanoparticles were measured in a standard optical setup with a back-scattering geometry. The laser excitation beam (λ=485 nm, 640 nm, or 405 nm) was focused, using a lens with a focal length of 30 mm, on the sample surface and the excitation power was controlled using notch filters. Typical excitation powers used were in the range of 200 μW. The emission was guided through a 150 μm pinhole and focused on a slit of a 0.5 monochromator (Shamrock 500, Andor) coupled with a charge coupled device detector (iDus 420BV, Andor). Fluorescence decays were studied using time-correlated single photon counting. For excitation, a diode-pumped solid state laser emitting at 405 nm, 640 nm, or 485 nm and generating 30 ps pulses at 80 MHz repetition rate was used. Detection was carried out with an ultrafast avalanche photodiode detector (idQuantique). The experiment was controlled using a time-correlated single photon counting card (SPC 150 Becker & Hickl). Emission spectra as well as fluorescence decays were collected for ten different spots across the sample in order to check for the reproducibility and homogeneity of the sample. Fluorescence of light-harvesting complexes was extracted using appropriate long-pass and band-pass optical filters.

2.4.1 Fluorescence imaging

In order to image fluorescence of light-harvesting complexes coupled to metallic nanoparticles we constructed a confocal fluorescence microscope based on Olympus infinity-corrected microscope objective LMPlan 50x, characterized with a numerical aperture of 0.5 and working distance of 6 mm (Krajnik, 2011). The resulting laser spot size is about 1 μm for the excitation laser of 485 nm. The sample is placed on a XYZ piezoelectric stage (Physik Instrumente) with 1 nm nominal resolution of a single step, which enables us to raster-scan the sample surface in order to collect fluorescence maps. They are formed by combining fluorescence intensity measurements with the motion of the XY translation stage. For excitation of fluorescence, we use one of four diode-pumped solid-state lasers with wavelengths of 405, 485, 532 and 640 nm. Typical optical power of the laser sources is about 5 mW, but in the case of actual measurements it needs to be strongly reduced in order to prevent photobleaching of the molecules. We used the excitation powers in the range of 0.004 to 0.04 mW. Gaussian beams of the lasers are achieved by using a spatial filter. The fluorescence is detected in a back-scattering geometry and focused on a confocal pinhole (150 μm) in order to reduce stray light coming out of the focal plane. The emission of PCP complexes is extracted with HQ 650LP (Chroma) dichroic mirror and HQ 670/10 (Chroma) bandpass filter. In order to extract fluorescence of LH2 complexes we used a longpass filter HQ850LP (Chroma) and a bandpass filter D880/40m (Chroma).

Our experimental configuration, described in detail in (Krajnik, 2011), allows for measuring fluorescence intensity, spectra and lifetimes. The spectrum, dispersed using the Amici prism is measured with a CCD camera (Andor iDus DV 420A-BV). The spectral resolution of the system is about 2 nm. Fluorescence intensity maps are collected with an avalanche photodiode (PerkinElmer SPCM-AQRH-14) with dark count rate of about 80 cps. Fluorescence lifetimes are measured using time-correlated single photon counting module (Becker & Hickl) equipped with fast avalanche photodiode (idQuantique id100-50) triggered by a laser pulse. Time resolution of the TCSPC setup is about 30 ps.

3. Experimental results

In this section we describe experimental results obtained for five architectures of hybrid nanostructures comprising metallic nanoparticles and light-harvesting systems. As for metallic nanostructures we used silver island film, semicontinuous silver film, spherical gold nanoparticles and elongated gold nanoparticles (nanorods). We coupled them with chlorophyll and carotenoid molecules embedded in the PCP complex from *Amphidinium carterae* and in the LH2 complex from *Rhodopseudomonas palustris*. The results of optical spectroscopy and microscopy show that the optical properties of light-harvesting systems are affected by the plasmon excitations in metallic nanoparticles both in th visible and infrared spectral ranges. Depending on the actual design of a nanostructure, either absorption or fluorescence radiative rate enhancement is obtained.

Generally, the effect of plasmon excitations in metallic nanoparticles on the optical properties of nearby emitters is monitored by measuring the fluorescence intensity. When the geometry of a hybrid nanostructure leads to plasmon-induced enhancement, the fluorescence intensity of such a hybrid structure is increased. When, on the other hand, non-radiative energy transfer from the emitter to the metallic nanoparticles plays the dominant

role, the emission is efficiently quenched. However, fluorescence spectrum alone gives only limited information about the actual processes responsible for the enhancement of the emission intensity. In order to elucidate the mechanisms in detail, it is important to combine standard fluorescence spectroscopy with fluorescence excitation spectroscopy and time-resolved fluorescence spectroscopy; these two experimental techniques provide a way to separate the plasmon-induced increase of the radiative rate from an induced increase of the absorption.

3.1 Peridinin-chlorophyll-protein on silver island film

Initial experiments on hybrid nanostructures composed of light-harvesting complexes and metallic nanoparticles have been carried out on PCP complexes deposited directly onto the silver island film layer (Mackowski, 2008). In order to change the spectral properties of the metallic film, we fabricated SIF substrates with 1 and 3 second long dipping time in the reaction solution. Next, PCP complexes diluted in PVA were spin coated in ensemble concentration on the SIF layer. Since the thickness of the PVA layer is approximately 100 nm, the structure formed in this way spans over all relevant ranges of plasmon-pigment interaction. For PCP complexes located very close to the SIF the non-radiative energy transfer to the metallic nanostructure should play a dominant role and thus fluorescence quenching is expected. In contrast, when the distance between light-harvesting complexes and the SIF is larger than 40-50 nm, there is virtually no interaction between the two components of the hybrid nanostructure. Yet, the optical properties of all in-between molecules should be affected by the plasmon excitations in metallic nanostructure.

In Fig. 7 we display fluorescence images obtained with our confocal fluorescence microscope for the PCP complexes spin-coated onto two SIF substrates characterized with different time of deposition. Bright areas correspond to the higher fluorescence intensity. In the case of the SIF substrate that was kept in the reaction solution for 1 minute only the image is relatively homogeneous, the variation of fluorescence intensity is moderate. On the other hand, for the second structure, which was kept in solution two minutes longer, the areas of high and low fluorescence intensity are clearly separated from each other. We attribute the areas characterized with high fluorescence intensity to regions where the SIF layer was formed during the reaction, while the low fluorescence intensity suggests that the metallic layer detached from the glass substrate during the reaction.

The structure where both SIF and glass surfaces are present at once provide an easy and straightforward means to compare the fluorescence properties of PCP complexes coupled to plasmon excitation to the uncoupled ones. In Fig. 8 we show fluorescence spectra as well as fluorescence decay curves measured with the laser focused on either one of the two areas. As expected, for the PCP complexes placed on the SIF substrate the intensity of the emission is substantially higher that for the reference structure. The enhancement factor estimated from these two spectra is about fourfold. It correspond well to the average enhancement factor obtained for this structure. Importantly, as demonstrated in previous report (Mackowski, 2008), the maximum emission of the PCP complexes as well as the shape of the fluorescence spectrum remain unchanged upon coupling the light-harvesting complexes to the metallic nanoparticles. Also, since we use a 485 nm laser wavelength for the excitation, the observation of the intact fluorescence emission for both substrates indicates that the efficiency of the energy transfer from carotenoids to Chl molecules is comparable. This

indicates that the PCP complexes that interact with metallic nanoparticles preserve their overall functionality. We can also see that the change in the fluorescence intensity is accompanied with sharp reduction of the fluorescence lifetime. In fact, the emission of PCP complexes on the glass substrate features a monoexponential decay while upon coupling to the SIF substrate the fluorescence decay curve is more complex. First a rapid decay takes place, which is probably due to efficient quenching of the PCP complexes that are very close to the metallic layer. After a first nanosecond the decay time of fluorescence gets longer, thus becoming similar to the decay observed for the reference structure.

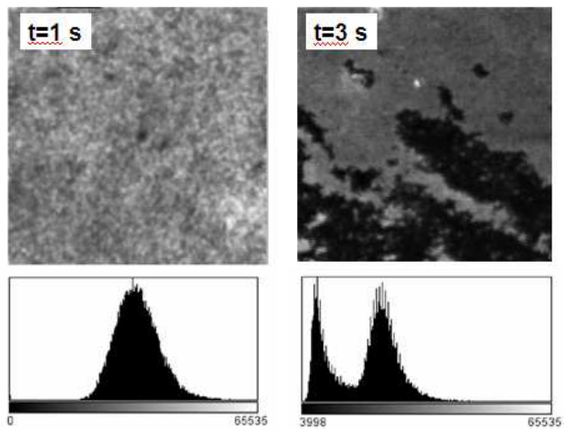

Fig. 7. Images of PCP fluorescence measured for the complexes deposited on the SIF substrate with 1 minute-long dipping time and 3 minute-long dipping time in the reaction solution. The maps were obtained at room temperature for the laser excitation wavelength of 485 nm, the laser power was 40 μW. The size of the images is 100x100 microns.

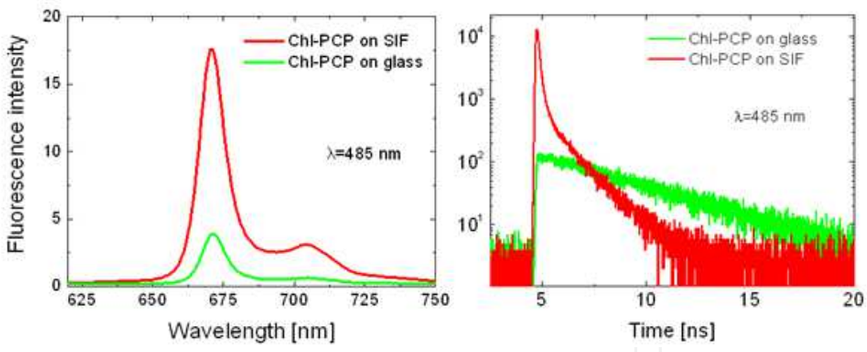

Fig. 8. Comparison between fluorescence spectra and fluorescence decay curves measured for PCP complexes on the glass and SIF substrates. For all measurements the excitation wavelength was 485 nm.

Overall, the results obtained for PCP complexes embedded in PVA matrix on the SIF layer demonstrate that high inhomogeneity of the structure leads to quite complicated behavior. Indeed the enhancement of absorption rate is entangled with enhancement of fluorescence rate, and in addition, signatures of non-radiative energy transfer from the chlorophylls to metallic structure are present. In the case of the hybrid nanostructure studied here, there is no control over the morphology of the SIF itself as well as over the separation between light-

harvesting complexes and metallic surface. Therefore, other approaches need to be devised, aimed at better control of sizes or shapes of metallic nanoparticles and the distance between the proteins and metallic structures.

3.2 Peridinin-chlorophyll-protein on semicontinuous silver film

In previous sections we pointed out the important role of the separation between light-harvesting complexes and the metallic nanoparticles. In the case of sample geometry involving inhomogeneous silver island film and PCP complexes spin-coated directly on top of it in a relatively thick PVA layer, we have observed that the increase of the fluorescence emission is a combined product of absorption and fluorescence rate enhancement. In addition, the signatures of non-radiative energy transfer from the PCP complexes to the SIF layer have been observed in the time-resolved spectra.

In order to minimize the influence of the processes that lead to fluorescence quenching and at the same time to achieve uniform distance from the metallic layer to light-harvesting complexes, we have fabricated a hybrid nanostructure based on semicontinuous silver film (Czechowski, 2011). Such a corrugated metallic surface can be made using e-beam assisted evaporation under high-vacuum conditions. Scanning electron microscopy studies of similarly prepared samples have indicated improved uniformity of the islands, that resulted in narrowing of the plasmon resonance measured in the absorption experiment (Chettiar 2010). Furthermore, on top of the silver film we deposited a 25-nm-thick silica layer. The layer serves two purposes: on the one hand it protects the silver surface against oxidation, on the other hand it provides a uniform spacer between metallic nanoparticles and light-harvesting complexes. The final change compared to the structure where PCP complexes were spin-coated in a PVA matrix on top of the SIF, concerned direct deposition of the PCP water solution on the SiO_2 surface of the spacer. In this way we can assume that all the complexes are at approximately identical distances from the silver islands. Here we used PCP complexes reconstituted with acChl a as they offer the largest energy separation between their fluorescence and plasmon resonance of silver islands. In addition, the concentration of PCP complexes is much higher than for samples prepared with spin-coating, which makes it possible to study the plasmon induced effects using standard fluorescence excitation spectroscopy.

The fluorescence excitation spectrum measured for the detection wavelength of 690 nm for acChl-PCP on glass substrate is shown in Fig. 9. It is compared with with the result obtained for acChl-PCP complexes placed on the semicontinuous silver film. The excitation spectrum for the reference structure is similar to previously published (Brotosudarmo, 2008) it features strong absorption due to Per in the spectral range from 400 nm to 550 nm, and corresponds roughly to the absorption spectrum. This suggests that the sample preparation leaves no effect on either the protein or the pigments. In contrast, the maximum of fluorescence excitation spectrum is blue-shifted by ~40 nm for the PCP complexes deposited on the silver island film and separated from the metallic nanostructures by a 25-nm thick SiO_2 layer. The difference between the two cases is seen after subtracting both curves and evaluating the enhancement of the emission. We find that the enhancement curve is a well-defined band with a maximum at 407 nm and linewidth of about 35 nm. We attribute this enhancement to plasmon excitations in the metallic layer that impact the absorption of the PCP complexes.

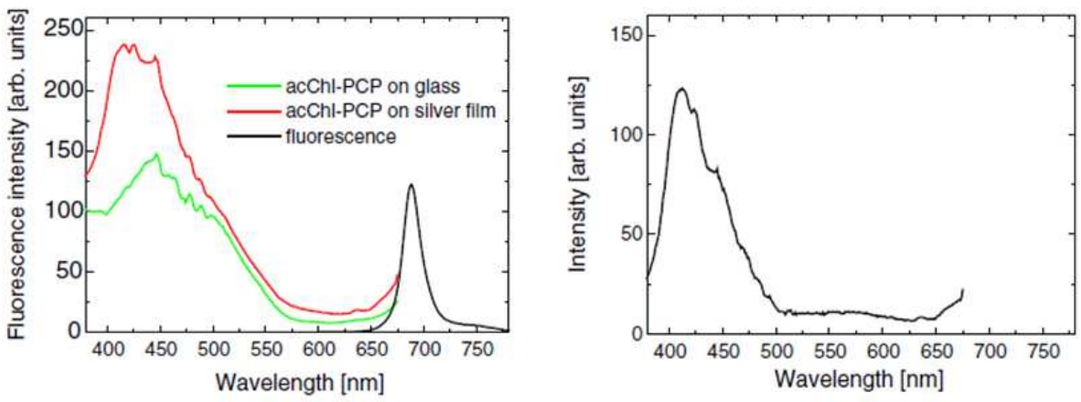

Fig. 9. Comparison between fluorescence excitation spectra measured for acChl-PCP on glass substrate and semicontinuous silver film. The detection energy was 690 nm. An enhancement dependence on the wavelength obtained by subtracting both fluorescence excitation curves is also shown.

It is important to note that the fluorescence excitation spectra measured for the reference structure and for the PCP complexes deposited on the silver film are not in any way adjusted or normalized. Yet, they are very comparable for wavelengths longer than 475 nm, in particular in the absorption range of low energy Per molecules. This suggests that the number of PCP complexes probed in both experiments is almost identical, which makes the estimation of the enhancement factor remarkably straightforward. Also the fluorescence spectrum measured for the hybrid nanostructure is is identical, for all excitation wavelengths, to that of the reference structure, which supports our previous observation that the preparation of the hybrid nanostructure has no measurable effect on the protein or pigment properties.

The fluorescence excitation data point towards increase of the absorption rate of the light-harvesting complex as being the dominant mechanism responsible for the enhancement of the fluorescence intensity. This suggestion is also helped with analysis of the spectral properties of both the PCP complexes and the semicontinuous silver film: they overlap mainly in the blue-green spectral range. In order to verify this we carry out time-resolved fluorescence experiment with the excitation wavelength of 405 nm, which corresponds to the maximum of the enhancement curve displayed in Fig. 9. The result if this experiment in shown in Fig. 10. The decay time of the control sample on glass is equal to 3.2 ns, while for the hybrid nanostructure a shortening of the lifetime to 2.3 ns when plasmons in the silver island film are excited. This less than 30 percent reduction of the lifetime, while measurable, is relatively small compared to previous results on fluorescent dyes (Dulkeith, 2002) and light-harvesting complexes (Mackowski, 2008), where order-of-magnitude changes have been measured. The small change of the fluorescence lifetimes in the case of the acChl-PCP complexes coupled to the semicontinuous silver film supports our conclusion that the enhancement measured in the fluorescence excitation is predominantly due to the enhancement of the excitation rate in the light-harvesting complexes. We also note that the fluorescence decay curve measured for the hybrid nanostructure features a monoexponential behavior, in contrast to the results obtained for PCP complexes deposited on the SIF. Such a uniform characteristics suggests improved homogeneity of the distance

between the light-harvesting complexes and the metallic layer, as indeed expected for our preparation procedure. We have also carried out time-resolved experiments with other excitation energies, in particular with 640 nm. This wavelength corresponds to direct excitation of Chl molecules and excites no plasmons. In this case the fluorescence decay shows no dependence upon either glass or metallic substrate.

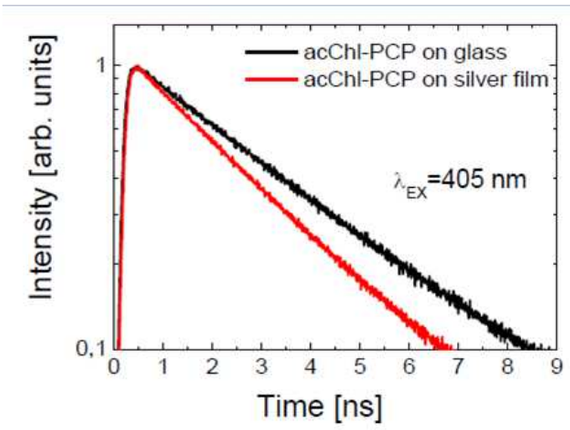

Fig. 10. Comparison of fluorescence decay curves measured for acChl-PCP on glass substrate and semicontinuous silver film. The excitation wavelength was 405 nm.

Finally we comment on another aspect of fluorescence decay time reduction observed for the 405 nm laser excitation. Since this reduction is attributed to the increase of the radiative rate of emission, it implies that there are plasmons excited in the semicontinuous silver film with wavelengths around 690 nm, where acChl-PCP emits. As 405 nm laser excites no such plasmons directly, this observation could be indicative of plasmon propagation in terms of energy relaxation. This hypothesis requires further experimental evidence but when proven correct, it could open another pathway in te field of plasmon engineering.

The results of fluorescence spectroscopy on acChl-PCP complexes deposited on semicontinuous silver film spaced by 25 nm SiO_2 layer confirm that by careful design of plasmonic hybrid nanostructure it is possible to selectively enhance the absorption of the light-harvesting complexes. The next step is to devise and fabricate a hybrid nanostructure, which would allow for systematic studies of plasmon induced effects as a function of the separation layer thickness.

3.3 Peridinin-chlorophyll-protein on spherical gold nanoparticles

The influence of the distance upon the interaction between PCP complexes and metallic nanoparticles requires fabrication of structures with precisely controlled thickness of the SiO_2 spacer. Such structures were fabricated in an analogous way as described previously, with the thickness of SiO_2 layer equal to 4, 12, and 40 nm. In this case however the metallic nanostructure used was a monolayer of uniform gold nanoparticles characterized with plasmon resonance at 530 nm.

While at the distances of 40 nm the influence of plasmon excitations on the optical properties of light-harvesting complexes is expected to be minimal, for thinner spacers the

effect should be much stronger. In order to evaluate that we carried out fluorescence imaging experiment on PCP complexes deposited on the three Au nanoparticle samples with varied thickness of the SiO_2 spacer. In the first step a fluorescence map was acquired of 100x100 micron sample area. The fluorescence maps were in all cases very uniform, variations of fluorescence intensity were below 15 percent. Next, approximately 50 fluorescence spectra we collected, each off a different spot on the sample surface. Finally, the same procedure was applied for measuring fluorescence decay curves. In this way statistically significant information about fluorescence intensity as well as fluorescence decay time is obtained.

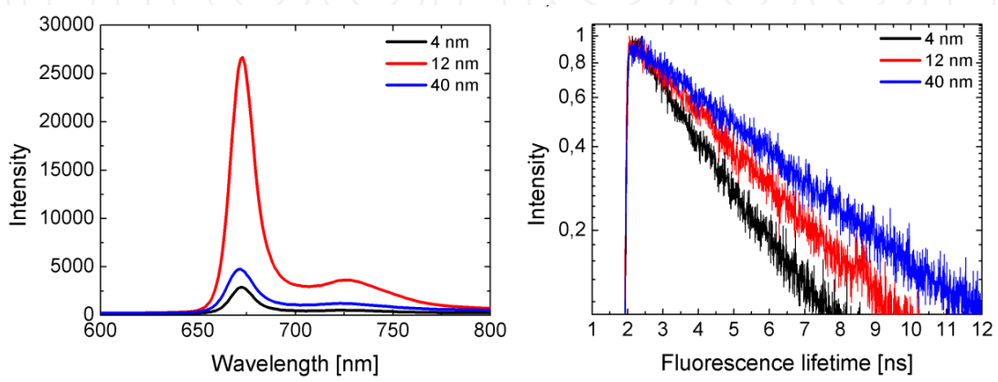

Fig. 11. Typical fluorescence spectra and fluorescence decay curves of Chl-PCP complexes deposited on Au nanoparticle substrates with different thickness of the SiO_2 spacer: 40 nm (blue), 12 nm (red), and 4 nm (black). The laser excitation wavelength was 485 nm.

In Fig. 11 we compare representative fluorescence spectra of Chl-PCP deposited on plasmonic substrates with Au spherical nanoparticles. The continuous-wave results are accompanied with time – resolved data. The intensity of fluorescence emission for 12 nm spacer is dramatically (fivefold) enhanced as compared to the reference structure with 40 nm thick SiO_2 spacer. For the smallest spacer (4 nm) the fluorescence decreases rapidly due to non-radiative energy transfer from chlorophylls embedded in the PCP complexes to metallic nanoparticles. Importantly, in analogy to all previously described experiments, the fluorescence spectrum of the light-harvesting complexes remains unchanged, indicating that the biomolecules are intact upon interacting with metallic nanoparticles.

Fluorescence decay curves that accompany the spectra provide means for understanding the mechanism of fluorescence enhancement. The decay time measured for the reference structure (40 nm) is equal to 3.3 ns, a typical value for PCP complexes reconstituted with Chl *a* (Mackowski, 2007). As the SiO_2 spacer gets thinner, the fluorescence lifetime gets shorter, and for 12 nm thick spacer is equal to 2.5 ns. Further reduction of the fluorescence lifetime is seen for the thinner, 4 nm, spacer. In this case the decay time is approximately 50 percent of the reference value. However, the mechanism of lifetime reduction is in both cases (4 nm and 12 nm) completely different. In the first case the shortening of the fluorescence decay time indicates enhancement of radiative rate of PCP complexes. This effects contributes to the observed increase of the emission intensity seen in the fluorescence spectra. On the other hand, for the 4 nm thick SiO_2 spacer, the lifetime reduction is due to excitation quenching. Thee results obtained for PCP complexes coupled to Au nanoparticles demonstrate clear

dependence of the fluorescence enhancement upon the distance between chlorophyll-containing proteins and metallic nanoparticles. While most of the effect is due to increase of absorption, there is also significant contribution associated with increase of the radiative rate. This approach can be then used for optimizing the geometry of plasmonic hybrid nanostructure for the most efficient performance.

3.4 Light-harvesting complex 2 on spherical gold nanoparticles

Light-harvesting complex LH2 from the purple bacteria is characterized by relatively weak absorption in the visible spectral range with its main absorption bands appearing in the near infrared, at 800 and 850 nm. By coupling LH2 to spherical gold nanoparticles we attempt to enhance the absorption between 400 and 550 nm. The geometry of the hybrid nanostructure was identical to discussed previously: monolayers of Au nanoparticles were covered with SiO_2 dielectric layers with thickness of 4, 12, and 40 nm. During the experiment the fluorescence spectra excited into carotenoid absorption (Wormke, 2007b) were measured at ten different locations across the sample. In this way it was possible to account for any inhomogeneities due to the preparation of the hybrid nanostructures. The fluorescence spectra measured with SiO_2 spacers between 4 and 40 nm and are shown in Fig. 12.

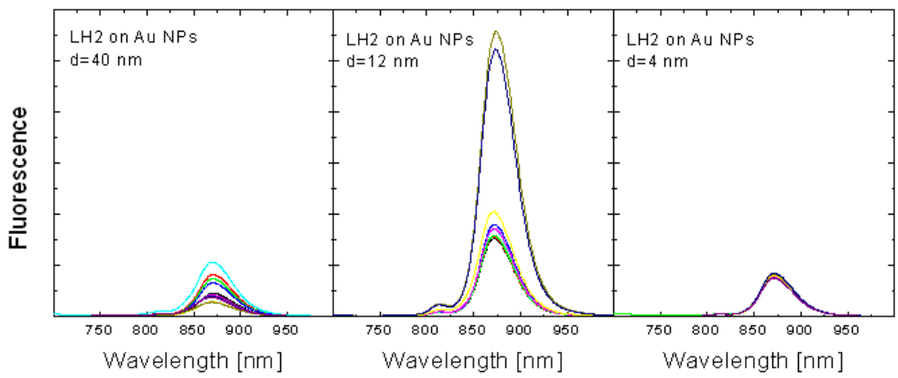

Fig. 12. Fluorescence spectra measured for LH2 complexes deposited on Au spherical nanoparticles on SiO2 spacers with thicknesses as indicated. The spectra were obtained for ten different locations on each sample.

There are several interesting observations worth pointing out. First of all, for the reference sample with 40-nm-thick SiO_2 spacer the scattering of the measured intensities can be attributed to local fluctuations in the LH2 concentration due to spin-coating approach. In contrast, for the sample with the 12-nm-thick SiO_2 spacer the spread of fluorescence intensities is significantly greater and the observed variation cannot be due to fluctuations of the LH2 concentration. Since plasmon interactions are expected to be significant for such a separation between the metallic nanoparticles and light-harvesting complexes, we attribute the distribution of fluorescence intensity to variation in plasmon coupling between the LH2 complexes and Au nanoparticles. Such variations can be caused for instance by interface roughness of the SiO_2 layer, even small variations of the spacer thickness would result in measurable changes of the fluorescence intensity. Finally, for the

thinnest SiO_2 layer of 4 nm the fluorescence intensities are all very similar. In fact, the measured distribution is even less pronounced than in the case of the reference sample. Such behavior may well be due to the dominant role of the fluorescence quenching caused by metallic nanoparticles, which takes over below a certain thickness of the spacer between the metallic nanoparticles and light-harvesting complexes. In such a case any fluctuations of either LH2 concentration or SiO_2 spacer thickness may be of lesser significance.

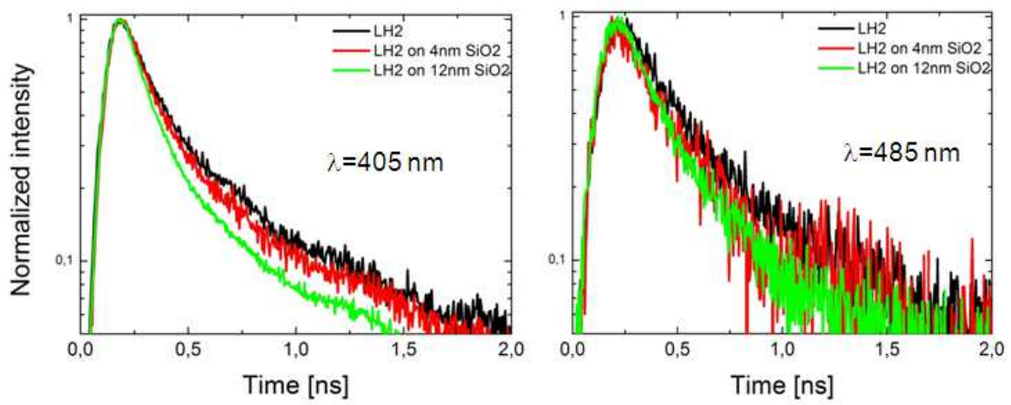

Fig. 13. Fluorescence decay curves measured for LH2 complexes on Au nanoparticles separated by SiO_2 spacer. Excitation wavelengths of 405 nm and 485 nm were used.

In order to determine the possible origin of the observed fluorescence enhancement, time-resolved fluorescence was measured on identically prepared samples. The fluorescence decay curves obtained for the structure with 4 and 12 nm thick SiO_2 layer is compared in Fig. 13 with the one measured for LH2 complexes deposited directly in glass substrate (Bujak, 2011). Apparently, upon coupling to the plasmons localized in the Au nanoparticles the fluorescence decays show virtually no change. Therefore, we assume that the fluorescence enhancement is predominantly due to an increase in the absorption in the carotenoid region of the LH2. The observation of exclusive increase of the absorption efficiency in the LH2 complexes coupled to Au nanoparticles was rendered by two factors. On the one hand, the difference in energy between plasmon resonance and the fluorescence emission is almost 400 nm, thus the overlap between low-energy tail of the plasmon resonance with the emission spectrum of the LH2 is minimal. This is much larger energy difference than for PCP complexes deposited on the semicontinuous silver film or Au nanoparticles. On the other hand, spherical gold nanoparticles are very uniform in size. This inhibits any possibility of energy relaxation in plasmonic structure, as it was observed for PCP complexes on the highly inhomogeneous SIF substrate.

The results described so far point clearly towards strong dependence of the plasmon induced effects upon the excitation energy. In most cases achieving strong coupling requires direct excitation of plasmons in metallic nanoparticles. In order to illustrate this, the fluorescence lifetimes were measured for LH2 complexes on Au nanoparticles with the excitation energy of 405 nm. In contrast to the 485 nm excitation, this energy excites

plasmons very inefficiently while still populating excited states of carotenoids. The results included in Fig. 13 show that the fluorescence lifetime shows no dependence upon the thickness of the SiO_2 spacer. However, the actual enhancement factor measured for 405 nm laser is substantially reduced compared to 485 nm laser, which very efficiently excites plasmons in metallic nanoparticles. The comparison is displayed in Fig. 14. For both excitation wavelengths the dependence of the enhancement factor on the distance between light-harvesting complexes and metallic nanoparticles is qualitatively the same. Yet, under the condition of efficient excitation of plasmons the maximum enhancement observed for the spacer with 12 nm thickness is 2.5 times greater.

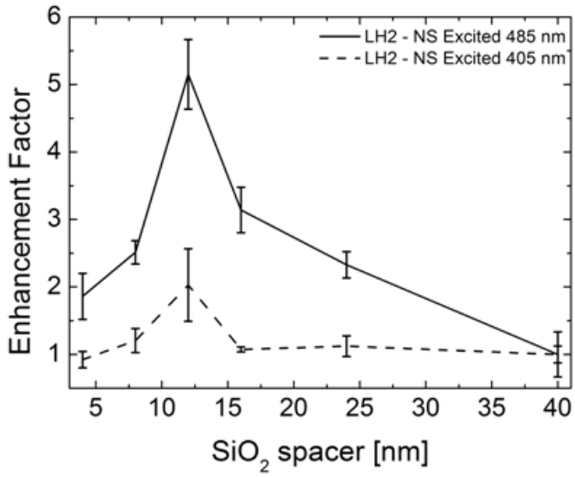

Fig. 14. Comparison of distance dependence of the fluorescence intensity enhancement for PH2 complexes deposited on Au spherical nanoparticles with different spacer thickness. The data was obtained for 485 nm and 405 nm laser excitations.

In conclusion, results of fluorescence spectroscopy carried out on hybrid nanostructures composed of light-harvesting complex LH2 and gold nanoparticles demonstrate the strong impact of plasmon excitations upon the optical properties of the biomolecule. For a spacer with a thickness of 12 nm substantial increase of the fluorescence intensity is observed, which is due to an enhancement of absorption of the carotenoids in this light-harvesting complex. Furthermore, we observe strong dependence of the fluorescence enhancement on the laser wavelength: for efficient excitation of plasmons in metallic nanoparticles (λ=485 nm) the enhancement is approximately 2.5 times stronger than for the out-of-plasmon-resonance excitation wavelength (λ=405 nm).

3.5 Light-harvesting complex 2 on gold nanorods

The final example of a hybrid nanostructure composed of light-harvesting complexes and metallic nanoparticles is a system where we combine Au nanorods with LH2 complexes from purple bacteria. From the previous discussion we know that by using Au nanorods we gain a tunability of plasmon resonances that reach near infrared spectral region (Bryant, 2008). In this way then we can affect the spectral properties of 800 and B850 absorption bands of the LH2 complex as well as its fluorescence emission.

In Fig. 15 we show the result of fluorescence imaging experiment carried out on LH2 complexes deposited directly on gold nanorods with plasmon resonances at 550 nm and 800 nm. The maxima of the resonances match ideally with absorption bands of the LH2 complex, attributed to carotenoids and bacteriochlorophylls, respectively. In the experiment we probe the fluorescence enhancement for these two excitation wavelengths, importantly for these two excitations the same sample area was monitored. It can be seen in particular for the maps shown in the upper row of Fig. 15, areas with low fluorescence intensity are clearly correlated. In the case of LH2 complexes on glass substrate fluorescence maps acquired for both excitation wavelengths are very uniform, as shown below the maps with intensity histograms. In both cases the histograms oare of Gaussian shape with maxima at 7500 and 21000 cps for 556 and 808 nm excitation, respectively. The picture changes

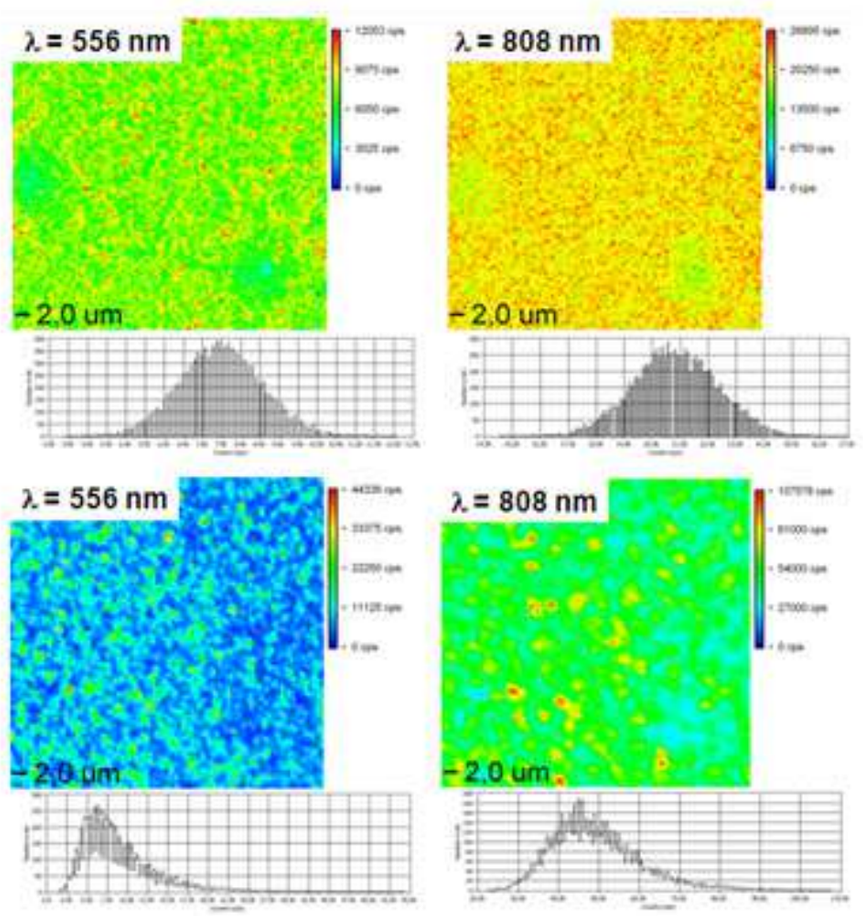

Fig. 15. Fluorescence images of LH2 complexes deposited on glass substrate (upper row) and Au nanorods (lower row). For exciting carotenoid absorption a 556 nm laser was used, whereas for exciting B800 BChl ring – a 808 nm laser was used. The maps for a given structure were obtained from the same sample area. The size of the images is 50 x 50 microns.

qualitatively for the LH2 complexes deposited on gold nanorods. The most pronouncing effect is much larger inhomogeneity of the fluorescence maps. There are regions of a few micron size that feature much stronger emission intensity. We can attribute them to either favorable separation between LH2 and Au nanorods or orientation/geometry of gold nanorods that would lead to formation of hot-spots of strongly localized electromagnetic field.

In addition to highly homogeneous fluorescence images, there are also significant differences of the distribution of fluorescence intensity, in spite of using the same excitation powers for a given laser wavelength. Indeed, the maximum of fluorescence intensity measured for 556 nm appears roughly at the same value as for the reference sample, but the histogram features substantial high-intensity tail of intensities, which is due to plasmon-induced enhancement in the hybrid nanostructure. Conversely, for the excitaiton of 808 nm the we also observe a broad tail towards higher intensities, but in this case the average intensity is also twice the average intensity measured for the reference sample. These preliminary results demonstrate that by using gold nanorods we are able to modulate the optical properties of multi-chromophoric systems such as light-harvesting complexes, which absorb in the infrared spectral range. Further work is required to coherently describe the complexity of plasmon interactions in this system.

4. Summary and conclusions

We have described various geometries of hybrid nanostructures composed of light-harvesting complexes from algae or purple bacteria and metallic nanostructures in the form of silver island films or monolayers of metallic nanoparticles synthesized chemically. The samples were studied with numerous optical spectroscopy and microscopy techniques including fluorescence excitation, time-resolved fluorescence, and fluorescence imaging with high spatial resolution. In all fabricated structures we observe strong effects attributable to plasmon induced effects on the optical properties of the light-harvesting complexes. Depending on the actual geometry we are able to increase fluorescence or absorption rate, in most cases however both effects are entangled. The results demonstrate that plasmon excitations in metallic nanostructures can be efficiently applied for controlling the light-harvesting capability of photosynthetic complexes, possibly paving the road towards novel photovoltaic architectures based – at least in some degree - on natural photosynthesis.

5. Acknowledgment

Research in Poland has been supported by the WELCOME project “Hybrid Nanostructures as a Stepping Stone towards Efficient Artificial Photosynthesis” funded by the Foundation for Polish Science and EUROCORES project “BOLDCATS” funded by the European Science Foundation. I am indebted to my friends and colleauges, with whom I have a great pleasure to collaborate on this project: I thank Wolfgang Heiss (Linz University), Eckhard Hofmann (University of Bochum), Richard J. Cogdell (University of Glasgow), Nicholas A. Kotov (University of Michigan), Hugo Scheer (LMU Munich) and the members of their research groups involved in parts of this research. Last but not least, I also acknowledge members of my research group at the Institute of Physics, Nicolaus Copernicus Unviersity in Torun, in

particular Dr. Dawid Piatkowski, Dr. Radek Litvin, Lukasz Bujak, Nikodem Czechowski, Bartosz Krajnik, Maria Olejnik, Kamil Ciszak, and Mikolaj Schmidt for their excellent work and vital contribution.

6. References

Akimoto, S.; Takaichi, S.; Ogata, T.; Nishimura, Y.; Yamazaki, I. & Mimuro, M. (1996), Excitation energy transfer in carotenoid chlorophyll protein complexes probed by femtosecond fluorescence decays, *Chemical Physics Letters*, Vol.260, No.1-2, (September 1996), pp.147-152, ISSN 009-2614

Anger, P; Bharadwaj, P. & Novotny, L. (2006), Enhancement and quenching of single-molecule fluorescence, *Physical Review Letters*, Vol.96, No. 11, (March 2006), pp. 113002, ISSN 0556-2813

Atwater, H & Polman, A.(2010), Plasmonics for improved photovoltaic devices, *Nature Materials*, Vol.9, (February 2010) pp. 205–213, ISSN 1476-1122

Blankenship, R. (2002), *Molecular Mechanisms of Photosynthesis*, Wiley-Blackwell, ISBN 978-0632-04321-7, Oxford, United Kingdom

Bopp, M.; Jia, Y.; Li, L.; Cogdell, R. & Hochstrasser R. (1997), Fluorescence and photobleaching dynamics of single light-harvesting complexes, *Proceedings of the National Academy of Sciences of the United States of America*, Vol.94, No.20, (September 1997), pp.10630-10635, ISSN *0027-8424*

Brotosudarmo, T.; Hofmann, E.; Hiller, R.; Wörmke, S.; Mackowski, S.; Zumbusch, A.; Bräuchle, C. & Scheer, H.(2006), Peridinin-chlorophyll-protein reconstituted with chlorophyll mixtures: preparation, bulk and single molecule spectroscopy, *FEBS Letters*, Vol.580, No.22, (October 2006), pp.5257–5262, ISSN 0014-5793

Brotosudarmo, T.; Mackowski, S.; Hofmann, E.; Hiller, R.; Bräuchle, C. & Scheer, H. (2008), Relative Binding Affinities of Chlorophylls in Peridinin - Chlorophyll - Protein Reconstituted with Heterochlorophyllous Mixtures, *Photosynthesis Research, Vol.*95, No.2-3, (February 2008), pp.247-252, ISSN 0166-8595

Bryant, G.; García de Abajo, F. & Aizpurua, J. (2008), Mapping the plasmon resonances of metallic nanoantennas, *Nano letters*, Vol.8, No.2, (January 2008), pp.631-636, ISSN 1530-6984

Bujak, L.; Czechowski, N.; Piatkowski, D.; Litvin, R.; Mackowski, S.; Brotosudarmo, T.; Cogdell, R.; Pichler, S. & Heiß, W. (2011), Absorption Enhancement of LH2 Light-Harvesting Complexes Coupled to Spherical Gold Nanoparticles, *Applied Physics Letters*, Vol.99, No.17, (October 2011), pp. 173701, ISSN 0003-6951.

Carmeli, I; Liberman, I.; Kraverski, L.; Fan, Z.; Govorov, A.; Markovich, G. & Richter, S. (2010), Broad band enhancement of light absorption in photosystem I by metal nanoparticle antennas, *Nano letters*, Vol.10, No.6, (May 2010), pp. 2069-2074, ISSN 1530-6984

Chettiar, U.; Nyga, P.; Thoreson, M.; Kildishev, A.; Drachev, V. & Shalaev, V. (2010), FDTD modeling of realistic semicontinuous metal films, *Applied Physics B: Lasers and Optics*, Vol.100, No.1, (March 2010), pp. 159-168, ISSN 1432-0649

Czechowski, N.; Nyga, P.; Schmidt, M.; Brotosudarmo, T.; Scheer, H.; Piatkowski D. & Mackowski, S. (2011), Absorption Enhancement in Peridinin-Chlorophyll-Protein

Light-Harvesting Complexes Coupled to Semicontinuous Silver Film, *Plasmonics*, Vol., (2011), pp.1-7, ISSN 1557-1955

Dulkeith, E.; Morteani, A.; Niedereichholz, T.; Klar, T.; Feldmann, J.; Levi, S.; van Veggel, F.; Reinhoudt, D.; Möller, M. & Gittins, D. (2002), Fluorescence quenching of dye molecules near gold nanoparticles: radiative and nonradiative effects, *Physical Review Letters*, Vol.89, No.20, (October 2002), pp.203002, ISSN 0556-2813

Govorov, A.; Bryant, G.; Zhang, W.; Skeini, T.; Lee, J.; Kotov, N.; Slocik, J. & Naik, R. (2006), Exciton−plasmon interaction and hybrid excitons in semiconductor−metal nanoparticle assemblies, *Nano letters*, Vol.6, No.5, (April 2006), pp. 984-994, ISSN 1530-6984

Govorov, A. (2008), Enhanced optical properties of a photosynthetic system conjugated with semiconductor nanoparticles: the role of Förster transfer. *Advanced Materials*, Vol.20, No.22, (April 2008), pp.4330-4335, ISSN 1521-4095

Hofmann, C.; Aartsma, T.; Michel, H. & Köhler, J. (2003), Direct observation of tiers in the energy landscape of a chromoprotein: a single-molecule study, *Proceedings of the National Academy of Sciences of the United States of America*, Vol.100, No.26, (December 2003), pp.15534-15538, ISSN *0027-8424*

Hofmann, E.; Wrench, P.; Sharples, F.; Hiller, R.; Welte, W. & Diederichs, K. (1996), Structural basis of light harvesting by carotenoids: peridinin-chlorophyll-protein from Amphidinium carterae, *Science*, Vol.272, No.5269, (June 1996), pp.1788–1791, ISSN 0036-8075

Hulteen, J. and van Duyne, R. (1995), Nanosphere Lithography: A Materials General Fabrication Process for Periodic Particle Array Surfaces, *Journal of Vacuum Science and Technology A,* Vol.13, No.3, (1995), pp.1553-1558, ISSN 0022-5355

Kim, I.; Bender, S.; Hranisavljevic, J.; Utschig, L.; Huang, L.; Wiederrecht, G. & Tiede, D. (2011), Metal nanoparticle plasmon-enhanced light-harvesting in a Photosystem I thin film, *Nano letters*, Vol.11, No.8, (August 2011), pp.3091-3098, ISSN 1530-6984

Kleima, F.; Hofmann, E.; Gobets, B.; van Stokkum, I.; van Grondelle, R.; Diederich, K. & van Amerongen, H. (2000), Förster excitation energy transfer in peridinin-chlorophyll a-protein, *Biophysical Journal*, Vol.78, No.1, (January 2000), pp.344–353, ISSN 0006-3495

Krajnik, B.; Schulte, T.; Piatkowski, D.; Czechowski, N.; Hofmann, E. & Mackowski, S. (2011), SIL-based Confocal Fluorescence Microscope for Investigating Individual Nanostructures, *Central European Journal of Physics*, Vol.9, No.2, (2011), 293-299, ISSN 1895-1082

Krueger, B.; Lampoura, S.; van Stokkum, I.; Papagiannakis, E.; Salverda, J.; Gradinaru, C.; Rutkauskas, D.; Hiller, R. & van Grondelle, R. (2001), Energy transfer in the peridinin chlorophyll-a protein of Amphidinium carterae studied by polarized transient absorption and target analysis, *Biophysical Journal*, Vol.80, No.6, (June 2001), pp.2843-2855, ISSN 0006-3495

Lakowicz, J. (2006), Plasmonics in biology and plasmon-controlled fluorescence, *Plasmonics*, Vol.1, No1., (2006), pp. 5-33, ISSN 1557-1955

Link, S. and El-Sayed, M. (1999), Size and Temperature Dependence of the Plasmon Absorption of Colloidal Gold Nanoparticles, *Journal of Physical Chemistry B*, Vol.103, No.21, (May 1999), pp.4212-4217, ISSN 1520-6106

Mackowski, S.; Wörmke, S.; Brotosudarmo, T.; Jung, C.; Hiller, R.; Scheer, H. & Bräuchle, C., *Biophysical Journal,* Vol. 93, No.9, (August 2007), pp. 3249-3258, ISSN 0006-3495

Mackowski, S.; Wörmke, S.; Maier, A.; Brotosudarmo, T.; Harutyunyan, H.; Hartschuh, A.; Govorov, A.; Scheer, H. & Bräuchle, C. (2008), Metal-enhanced fluorescence of chlorophylls in single light - harvesting complexes, *Nano letters*, Vol.8, No.2, (February 2008), pp. 558-564, ISSN 1530-6984

Mackowski, S. (2010), Hybrid Nanostructures for Efficient Light Harvesting, *Journal of Physics: Condensed Matter, Vol.*22, No.19, (April 2010), pp.193102/1-17, ISSN 0953-8984

Maier, S. (2004). *Plasmonics: fundamentals and applications,* Springer Science + Business Media LLC, ISBN 978-0387-37825-1, New York, USA

McDermott, G.; Prince, S.; Freer, A.; Hawthornthwaite-Lawless, A.; Papiz, M.; Cogdell, R. & Isaacs, N. (1995), Crystal structure of an integral membrane light-harvesting complex from photosynthetic bacteria, *Nature*, Vol.374, (April 1994), pp. 517-521, ISSN 0028-0836

Nieder, J.; Bittl, R. & Brecht, M. (2010), Fluorescence studies into the effect of plasmonic interactions on protein function, *Angewandte Chemie International Edition*,Vol.49, No.52, (November 2010), pp. 10217–10220, ISSN 1521-3773

Polivka, T. & Sundström, V. (2004), Ultrafast dynamics of carotenoid excited states-from solution to natural and artificial system, *Chemical Reviews*, Vol.104, No.4, (February 2004), pp.2021–2071, ISSN 0009-2665

Polívka, T.; Pascher, T.; Sundström, V. & Hiller, R. (2005), Tuning energy transfer in the peridinin-chlorophyll complex by reconstitution with different chlorophylls, *Photosynthesis Research*, Vol.86, No.1-2, (2005), pp.217-227, ISSN 0166-8595

Ray, K.; Badugu, R. & Lakowicz, J. (2006), Metal-Enhanced Fluorescence from CdTe Nanocrystals: A Single-Molecule Fluorescence Study, *Journal of American Chemical Society,* Vol.128, No.28, (June 2006), pp.8998-8999, ISSN 0163-3864

Scheuring, S.; Sturgis, J.; Prima, V.; Bernadac, A.; Lévy, D. and Rigaud. J. (2004), Watching the photosynthetic apparatus in native membranes, *Proceedings of the National Academy of Sciences of the United States of America,* Vol.101, No.31, (August 2004), pp.11293-11297, ISSN 0027-8424

van Oijen, A.; Ketelaars, M.; Köhler, J.; Aartsma T. & Schmidt, J. (1999), Unraveling the electronic structure of individual photosynthetic pigment-protein complexes, *Science*, Vol.285, No.5426, (July 1999), pp.400-402, ISSN 0036-8075

Wörmke, S.; Mackowski, S.; Jung, C.; Ehrl, M.; Zumbusch, A.; Brotosudarmo, T.; Scheer, H.; Hofmann, E.; Hiller R. & Bräuchle, C. (2007a), Monitoring Fluorescence of Individual Chromophores in Peridinin-Chlorophyll-Protein Complex Using Single Molecule Spectroscopy, *Biochimica et Biophysica Acta – Bioenergetics,* Vol.1767, No.7, (July 2007), pp.956-964, ISSN 0006-3002

Wörmke, S.; Mackowski, S.; Brotosudarmo, T.; Garcia, T.; Braun, P.; Scheer, H.; Hofmann, E. & Bräuchle, C. (2007b), Detection of single biomolecule fluorescence excited

through energy transfer: Application to light-harvesting complexes, *Applied Physics Letters*, Vol.90, No.19, (May 2007), pp.193901, ISSN 0003-6951

Wörmke, S.; Mackowski, S.; Schaller, A.; Brotosudarmo, T.; Johanning, S.; Scheer, H. & Bräuchle C. (2008), Single Molecule Fluorescence of Native and Refolded Peridinin-Chlorophyll-Protein Complexes, *Journal of Fluorescence*, Vol.18, No. 3-4, (2008), pp. 611-617, ISSN 1053-0509

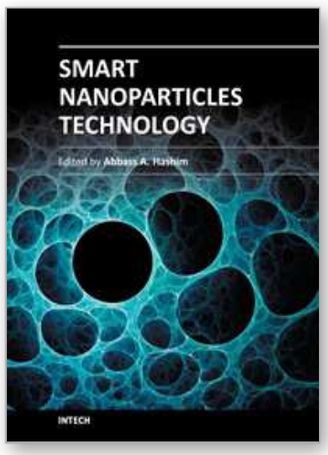

Smart Nanoparticles Technology

Edited by Dr. Abbass Hashim

ISBN 978-953-51-0500-8
Hard cover, 576 pages
Publisher InTech
Published online 18, April, 2012
Published in print edition April, 2012

In the last few years, Nanoparticles and their applications dramatically diverted science in the direction of brand new philosophy. The properties of many conventional materials changed when formed from nanoparticles. Nanoparticles have a greater surface area per weight than larger particles which causes them to be more reactive and effective than other molecules. In this book, we (InTech publisher, editor and authors) have invested a lot of effort to include 25 most advanced technology chapters. The book is organised into three well-heeled parts. We would like to invite all Nanotechnology scientists to read and share the knowledge and contents of this book.

How to reference

In order to correctly reference this scholarly work, feel free to copy and paste the following:

Sebastian Mackowski (2012). Metallic Nanoparticles Coupled with Photosynthetic Complexes, Smart Nanoparticles Technology, Dr. Abbass Hashim (Ed.), ISBN: 978-953-51-0500-8, InTech, Available from: http://www.intechopen.com/books/smart-nanoparticles-technology/metallic-nanoparticles-coupled-to-photosynthetic-complexes

INTECH
open science | open minds

InTech Europe
University Campus STeP Ri
Slavka Krautzeka 83/A
51000 Rijeka, Croatia
Phone: +385 (51) 770 447
Fax: +385 (51) 686 166
www.intechopen.com

InTech China
Unit 405, Office Block, Hotel Equatorial Shanghai
No.65, Yan An Road (West), Shanghai, 200040, China
中国上海市延安西路65号上海国际贵都大饭店办公楼405单元
Phone: +86-21-62489820
Fax: +86-21-62489821

IntechOpen